

Electronic structure of cubic gallium nitride films grown on GaAs

Cite as: Journal of Vacuum Science & Technology A **14**, 819 (1996); <https://doi.org/10.1116/1.580396>
 Submitted: 09 November 1995 • Accepted: 28 December 1995 • Published Online: 04 June 1998

S. A. Ding, G. Neuhold, J. H. Weaver, et al.



View Online



Export Citation

ARTICLES YOU MAY BE INTERESTED IN

Valence band discontinuity at a cubic GaN/GaAs heterojunction measured by synchrotron-radiation photoemission spectroscopy

Applied Physics Letters **70**, 2407 (1997); <https://doi.org/10.1063/1.118886>

Lattice parameters of gallium nitride

Applied Physics Letters **69**, 73 (1996); <https://doi.org/10.1063/1.118123>

Quantum confinement effect in self-assembled, nanometer silicon dots

Applied Physics Letters **73**, 3881 (1998); <https://doi.org/10.1063/1.122923>

HIDEN
ANALYTICAL

Instruments for Advanced Science

- Knowledge,
- Experience,
- Expertise

Click to view our product catalogue

Contact Hiden Analytical for further details:

W www.HidenAnalytical.com

E info@hiden.co.uk

Gas Analysis

- ▶ dynamic measurement of reaction gas streams
- ▶ catalysis and thermal analysis
- ▶ molecular beam studies
- ▶ dissolved species probes
- ▶ fermentation, environmental and ecological studies

Surface Science

- ▶ UHVTPD
- ▶ SIMS
- ▶ end point detection in ion beam etch
- ▶ elemental imaging - surface mapping

Plasma Diagnostics

- ▶ plasma source characterization
- ▶ etch and deposition process reaction kinetic studies
- ▶ analysis of neutral and radical species

Vacuum Analysis

- ▶ partial pressure measurement and control of process gases
- ▶ reactive sputter process control
- ▶ vacuum diagnostics
- ▶ vacuum coating process monitoring



Electronic structure of cubic gallium nitride films grown on GaAs

S. A. Ding, G. Neuhold, J. H. Weaver,^{a)} P. Häberle,^{b)} and K. Horn^{c)}
Fritz-Haber-Institut der Max-Planck-Gesellschaft, D-14195 Berlin, Germany

O. Brandt, H. Yang, and K. Ploog
Paul-Drude-Institut für Festkörperelektronik, D-10117 Berlin, Germany

(Received 9 November 1995; accepted 28 December 1995)

The composition, surface structure, and electronic structure of zinc blende-GaN films grown on GaAs (100) and (110) by plasma-assisted molecular beam epitaxy were investigated by means of core and valence level photoemission. Angle-resolved photoelectron spectra (photon energy 30–110 eV) exhibited emission from the Ga 3*d* and N 2*s* levels, as well as a clear peak structure in the valence band region. These peaks were found to shift with photon energy, indicative of direct transitions between occupied and unoccupied GaN bands. By using a free electron final band, we are able to derive the course of the bands along the Γ -*X* and Γ -*K-X* directions of the Brillouin zone and to determine the energy of critical points at the *X* point. The relative energies of the Ga 3*d* and nitrogen 2*s* bands were also studied, and a small amount of dispersion was detected in the latter. The resulting band structure is discussed in relation to existing band structure calculations. © 1996 American Vacuum Society.

I. INTRODUCTION

The group III nitrides have received renewed attention in recent years because of their potential for short-wavelength optoelectronic applications, as demonstrated by the implementation of efficient blue light-emitting diodes.¹ These materials, with their direct band gaps of 6.2 eV (AlN), 3.4 eV (GaN), and 1.9 eV (InN), offer the possibility of tailoring the photoresponse or emitted wavelength through alloying. High quality bulk samples are difficult to produce. Most studies thus deal with thin films grown on either SiC or sapphire. Progress has recently been made in preparing thin films of GaN on gallium arsenide surfaces by plasma-assisted molecular beam epitaxy (MBE),^{2,3} metalorganic vapor-phase epitaxy (MOVPE),⁴ and similar techniques, which is surprising in view of the large (20%) lattice mismatch between these materials.

While the lowest energy structure of the group III nitrides is the hexagonal (wurtzite) phase, it was recently demonstrated that cubic GaN films can also be grown (see Ref. 5, and references therein), although it seems that the hexagonal phase often coexists with the cubic one. Recently, Brandt *et al.*⁵ have demonstrated that purely cubic GaN films of high quality can be grown on GaAs (100), which the authors ascribe to a control of surface stoichiometry. They have also succeeded⁶ in stabilizing cubic GaN (110) films on GaAs (110) substrates having a similar quality as the GaN (100) films. The resulting GaN films are stable in air, and after exposure to air the clean surface can be recovered by heating in ultrahigh vacuum to about 700 °C. This offers the possi-

bility to study cubic GaN by surface spectroscopies and other experimental methods. Here we report a study of the electronic band structure of (100)- and (110)-oriented films of cubic GaN films using angle-resolved photoelectron spectroscopy along the (001) and (110) crystallographic directions.

II. EXPERIMENT

The experiments were carried out in an angle-resolved photoelectron spectrometer (ADES 400, VG Scientific, UK) with a base pressure of 1×10^{-10} mbar that was equipped with a sample introduction lock, sample heating and cooling facilities, low energy electron diffraction (LEED) optics, and a moveable hemispherical electron energy analyzer. Photoelectrons were excited by light from the BESSY (Berliner Elektronen-Speicherring-Gesellschaft für Synchrotronstrahlung) storage ring and dispersed by the toroidal grating monochromators TGM 4 and TGM 6. GaN (100) and (110) samples that were grown by plasma-assisted MBE on *n*-type GaAs (100) and (110) substrates in a separate chamber⁵ were loaded into the vacuum chamber after a brief etch in HCl with subsequent rinsing in distilled water. Clean surfaces were prepared by annealing to 700 °C. The surfaces were found to be free from contaminating species such as oxygen or carbon as determined from a separate x-ray photoelectron spectroscopy experiment where the intensity of the C 1*s* and O 1*s* lines was measured before and after heating. Annealing resulted in (1×1) LEED patterns with a rather high diffuse background. The surface Fermi level after annealing was about 1.2 eV above the valence band maximum in both GaN (100) and (110) films.

III. RESULTS AND DISCUSSION

The valence level spectrum from the valence band maximum (VBM) down to the region about 4 eV below the gal-

^{a)}Permanent address: Department of Chemical Engineering and Materials Science, University of Minnesota, Minneapolis, MN 55455.

^{b)}Permanent address: Departamento de Física, Universidad Técnica Federico Santa María, Valparaíso, Chile.

^{c)}Author to whom correspondence should be addressed; mailing address: Fritz-Haber-Institute, Faradayweg 4-6, D-14195 Berlin, Germany; electronic mail: horn@fhi-berlin.mpg.de

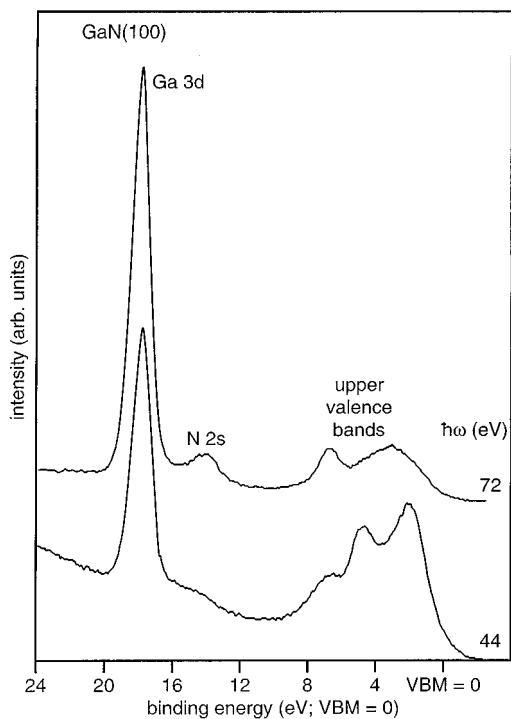


FIG. 1. Comparison of valence band spectra of GaN (100) from the valence band maximum to the Ga 3*d* region for photon energies of 44 and 72 eV. Note the emergence of the N 2*s* peak in the top spectrum.

limum 3*d* level is shown for a clean surface of GaN (100) in Fig. 1, recorded in normal emission at photon energies of 44 and 72 eV. The region down to about 8 eV below the VBM is characterized by three closely spaced peaks that correspond to the Ga *s-p*/N *p*-derived valence bands. These peaks exhibit clear changes in intensity and position with photon energy by comparison between the lower and the upper spectrum. The intense peak at a binding energy of 17.7 eV below the VBM is due to the Ga 3*d* core level. In the region between the valence bands and the 3*d* peak, a broad peak is seen close to the Ga 3*d* peak in the spectrum at 44 eV photon energy, which develops into a clearly separated peak at 72 eV photon energy. This peak is due to the nitrogen 2*s* level at a binding energy of 14.2 eV below the VBM. The binding energies of the Ga 3*d* and N 2*s* peaks are similar to those observed in an angle-integrated photoemission study of wurtzite GaN (0001) by Hunt *et al.*⁷ As will be discussed in more detail below, all of these peaks form part of the electronic structure that must be considered in a treatment of the valence bands.

The experimental determination of electronic band structures⁸ by angle-resolved photoemission, which has been an important tool for the study of the electronic structure of a wide variety of solids, is based on the determination of photoelectron momentum in *k*-conserving band-to-band transitions. Electron momentum can be varied through a choice of emission angle and electron kinetic energy according to the free electron energy–momentum relation $E_{\text{kin}} = \hbar^2 k^2 / 2m_{\text{el}}$, where *k* is the electron wave vector and m_{el} its

mass. In a direct transition from an occupied to an unoccupied band, the momentum of the electron in the final state $\mathbf{k}_{\text{final}}$ is related to the momentum in the initial state $\mathbf{k}_{\text{initial}}$ as follows. The component of momentum parallel to the surface k_{\parallel} is conserved modulo a reciprocal lattice vector in the photoemission process, whereas the normal component k_{\perp} is affected by the potential step at the surface, which is taken into account by introducing an “inner potential” V_0 , that defines the zero of energy for the free electron final state and is subtracted when evaluating the electron momentum normal to the surface through

$$k_{\text{final}} = \frac{\sqrt{2m_{\text{el}}}}{\hbar} \sqrt{E_{\text{kin}} + V_0}. \quad (1)$$

This simple approach, which amounts to taking a free electron parabola as the final band, has yielded remarkable success in the evaluation of band structures of metals and semiconductors and is the basis for an evaluation when calculations of final bands are not available, as in the present case. Often, normal emission spectra, corresponding to $k_{\parallel} = 0$, from low index faces are recorded for a wide range of photon energies such that only k_{\perp} is changed along a particular line of high symmetry in the three-dimensional Brillouin zone (BZ). This procedure, which necessitates the use of synchrotron radiation, provides a test of the validity of the above approach since the influence of direct transitions on the valence band spectrum can be identified through a continuous shift of peaks with photon energy. This is readily seen for strongly dispersing peaks.

In order to systematically analyze the changes in energy of the topmost valence band peaks, let us consider the set of valence band spectra (excluding Ga 3*d* and nitrogen 2*s*), recorded from GaN (001) and shown in Fig. 2. Three separate peaks are visible at intermediate photon energies, e.g., at 38–44 eV. Except for the peak at highest binding energy (about 6 eV), all peaks exhibit clear shifts in energy. Binding energies in photoelectron spectra from semiconductors are usually related to the VBM, which is determined by extrapolating the main low binding energy slope of the leading peak to zero intensity, for example, in the spectrum at 31 eV. The problem when using such binding energy values for band structure determinations is that the volume of states in *k* space becomes infinitesimally small as one approaches the Γ point, such that band-to-band transitions are only detected close to this point due to the limited energy and angular resolution as well as initial and final state broadening. Thus the intercept of the tangent to the leading peak is chosen as the zero of binding energies, e.g., when referencing the binding energy of core levels, while the valence band maximum for the band structure diagrams (Figs. 4 and 6) is referenced with respect to the leading peak position for photon energies near the Γ point (see below), which differ by 1.1 eV in the present case.

Appreciable intensity in the spectra occurs even above the extrapolated leading edge, extending about 1.6 eV into the band gap, which is most likely related to defect-induced states caused by disorder on the surface. The peak at highest

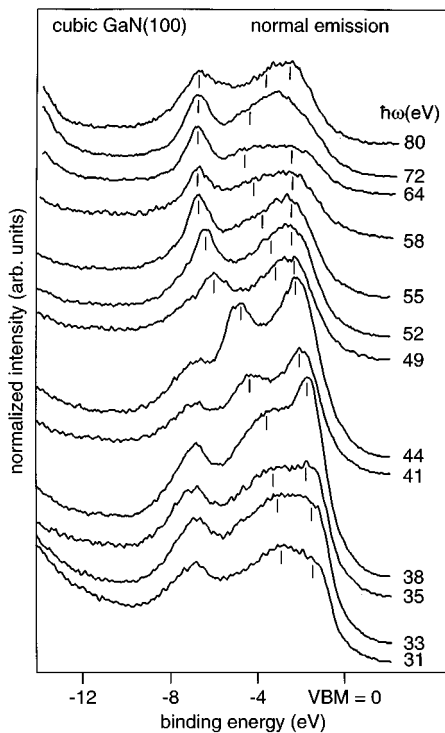


FIG. 2. Set of valence band spectra from GaN (100), recorded in normal emission for photon energies from 31 to 80 eV. Peak positions used in band determinations are indicated by markers underneath each spectrum. The location of the VBM was evaluated from an extrapolation of the leading edge of the spectrum.

binding energy (approximately 6.8 eV) consists of a stationary part and a superimposed dispersing peak, most clearly seen in the spectra at 49, 52, and 55 eV. The structure most difficult to follow by direct inspection is the one between the topmost peak and the peak at 6.7 eV. However, it can be distinguished as a filling up of the valley and a broadening of the leading peak. The overall width of the upper valence band range is similar to the width of the emission in this range in angle-integrated spectra from wurtzite-GaN (0001) reported by Hunt *et al.*⁷

In the extended Brillouin zone scheme, the line Γ - X - Γ is sampled when analyzing normal emission spectra from a cubic (100) surface. For the range of photon energies used in our experiments (31–99 eV) and a value for the inner potential of $V_0=10$ eV, the values for k_{\perp} range from 3.27 to 5.32 \AA^{-1} . Based on the lattice constant of cubic GaN of 4.52 \AA , this means that the Γ point is reached at k_{\perp} values of 2.78 and 5.56 \AA^{-1} , while the X point is reached at 4.17 \AA^{-1} , i.e., at a photon energy of about 77 eV for X_5 ; here the binding energy of all three peaks has its maximum as expected. Along the Γ - K - X direction, the X point is reached at $k_{\perp}=1.97$ \AA^{-1} , K at 2.47 \AA^{-1} , Γ at 3.94 \AA^{-1} , and K again at 5.88 \AA^{-1} . Spectra along this direction were recorded through normal emission from the (110) oriented GaN film for a range of photon energies from 25 to 110 eV, corresponding to k_{\perp} values from 3.02 to 5.59 \AA^{-1} . These spectra are shown in Fig. 3. The spectra are somewhat less structured than those from the (100) oriented GaN film, but several features can be

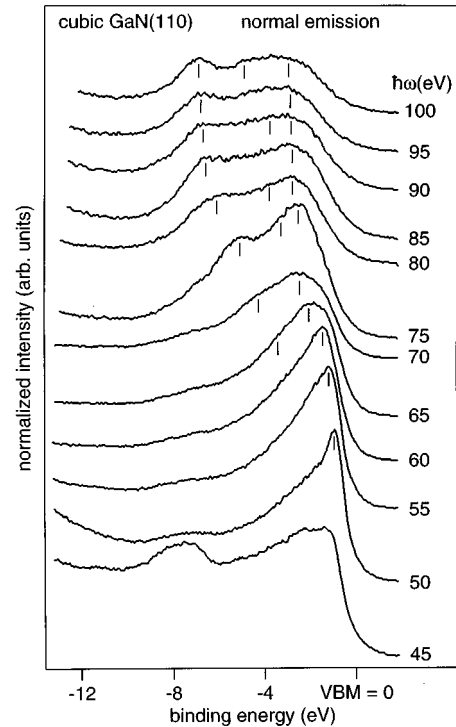


FIG. 3. Set of valence band spectra from GaN (110), recorded in normal emission for photon energies from 45 to 100 eV.

clearly seen just as well. At photon energies around 50 eV where, according to the evaluation of electron wave vectors above, the Γ point is reached, a sharp and asymmetric peak close to the VBM dominates the spectrum. This shifts to lower energies. A second peak at higher binding energy develops for increasing photon energies and disperses to a final binding energy of about 6.7 eV below the VBM. Finally, a third peak can be seen as a shoulder (spectrum at 100 eV) between the top and bottom peaks.

The experimental band structure can now be evaluated from the energies of peaks in the spectra in Figs. 2 and 3, based on the free electron final state formula. This is shown in Fig. 4 for the Γ - X and Γ - K - X directions. Each datum point corresponds to a peak position in one of the spectra. The lines indicating the dispersion of the different bands are from a calculated band structure of cubic GaN by Fiorentini, Methfessel, and Scheffler.⁹ As is evident from a comparison of the experimental and theoretical data in Fig. 3, there is reasonable agreement between the results of the evaluation of the angle-resolved photoelectron spectra and the calculations as far as the strongly dispersing Δ_1 band along Γ - X is concerned. Except for two data points near the VBM that arise from spectra at lower photon energy, the theoretical curve matches the experimental data points. This agreement can in part be improved by adjusting the inner potential V_0 . Instead of performing this adjustment by eye, the strongly dispersing theoretical Δ_2 band was approximated by a fourth-order polynomial, and the agreement between the data points and this band was optimized by means of a least-squares

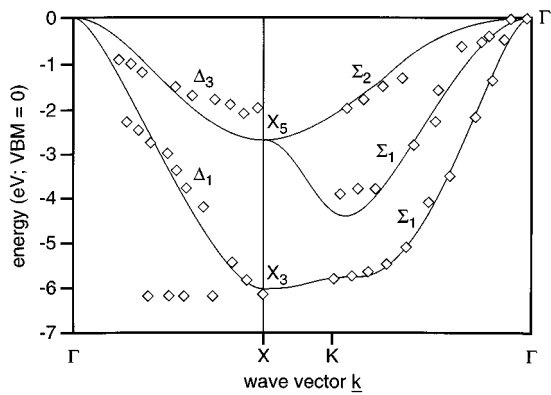


FIG. 4. Experimental band structure of *c*-GaN along the Γ -X and Γ -K-X directions in the Brillouin zone; single group symmetry labels are used throughout. Diamonds indicate the location of peaks in the spectra, where the magnitude of the \mathbf{k} vector was evaluated based on a free electron final state (see the text). Energy scale has been adjusted to zero for transitions at the Γ point.

method with V_0 as a free parameter. A value for $V_0=10.4$ eV was thus obtained and was used in all further evaluations.

The peak at about 6.7 eV that does not exhibit dispersion is due to indirect emission from the high density of states near the X_3 point. A stationary peak in this region is generally found in photoemission spectra from III-V semiconductors.¹⁰⁻¹² Agreement is slightly worse for the upper Δ_3 band. Here the data indicate a dispersion that is smaller than the calculated one by about 0.7 eV, with a value for the X_5 point of 2.0 eV. This value will be compared with other existing band structure calculations in Table I below. There is also some deviation at small k_{\perp} values that may be connected to the problem of finding the band location close to the VBM near Γ . For the Γ -K-X direction, good agreement is also found. Unfortunately, due to the limitations of the monochromator, it was not possible to use photon energies high enough in order to reach the X point along the Γ -K-X and thus to provide an independent test of the X point energies. However, calculated second and third Σ_1 and Σ_2 bands closely match the experimental data points, although for the lower band the data would indicate a rather

stronger dispersion at small k_{\perp} values. The topmost band is only represented by a few data points because of the width of the peaks and the overlap with other features.

The energies of critical points and their comparison with calculations are the most important results of the experimental band structure determination. One has to distinguish between those calculations which treat the Ga 3*d* electrons as inert core electrons and those which explicitly include them. It has been shown that, because of the close proximity of the Ga 3*d* and N 2*s* levels, hybridization occurs and, consequently, these levels have to be considered on an equal footing with the other valence electrons.⁹ We thus restrict our comparison with the calculations to those that include the Ga 3*d* levels.^{9,13-16} Values from these calculations are collected for the lowest *s* band and the upper bands in Table I. The general agreement between the different calculations is adequate and, apart from the band energy at X_5 , also between the calculations and experiment. For the latter, all calculations give a dispersion consistently larger by about 0.7 eV than our experimental results, such that a lack of resolution of the top band within the peak near the VBM may be blamed for this discrepancy, which may be improved once a better sample preparation procedure is available.

The behavior of the lower Ga 3*d* and N 2*s* states has received particular attention in view of the proximity of the N 2*s* and Ga 3*d* levels that are expected to lead to strong hybridization. A close-up set of spectra of this region is shown in Fig. 5. The Ga 3*d* peak is rather featureless and shows very little change when excited with different photon energies. The smaller peak, shown enlarged, exhibits an intensity maximum with increasing photon energies and also suggests a small amount of energy shift with photon energy. Since this is difficult to determine in a small peak adjacent to a strong feature, a series of line shape analyses based on least-squares (χ^2) optimization was carried out for this set of spectra; an example of this is found in the bottom spectrum. Here, Lorentzians convoluted by a Gaussian were used to model both the Ga 3*d* and the N 2*s* peaks, and a second-

TABLE I. Critical points in the cubic GaN band structure from different calculations, compared with results from angle-resolved photoemission (this work).

Critical point	Ga 3 <i>d</i> -N 2 <i>s</i> derived		Ga 4 <i>s</i> /4 <i>p</i> -N 2 <i>p</i> derived		Band energies at the K point		
	Γ_{1v}	X_{1v}	X_1	X_4	Lowest	Center	Upper
Rubio <i>et al.</i> (Ref. 13)	-16.3 (LDA)	-13.0 (LDA)	-6.5 (LDA)	-2.8 (LDA)	-6.2 (LDA)	-4.7 (LDA)	-2.8 (LDA)
	-17.8 (GW)	-14.8 (GW)	-6.9 (GW)	-3.0 (GW)			
Fiorentini <i>et al.</i> (Ref. 9)	-15.64	-13.73	-6.02	-2.67	-5.73	-4.39	-1.95
Wenchang <i>et al.</i> (Ref. 15)	-16.0	-10.7	-6.0	-2.8	-5.75	-4.6	-2.7
Wright and Nelson (Ref. 14)	-15.0	-11.3	-6.2	-2.7	-6.0	-4.5	-2.2
Christensen and Gorczyca (Ref. 16)	-15.7	-12.7	-6.5	-2.7	-5.5	-4.5	-2.0
Lambrech <i>et al.</i> (Ref. 17)	-13.3		-6.0				
Experimental results (this work)	-12.5	-11.85	-6.1	-2.0	-5.8	-4.0	2.1

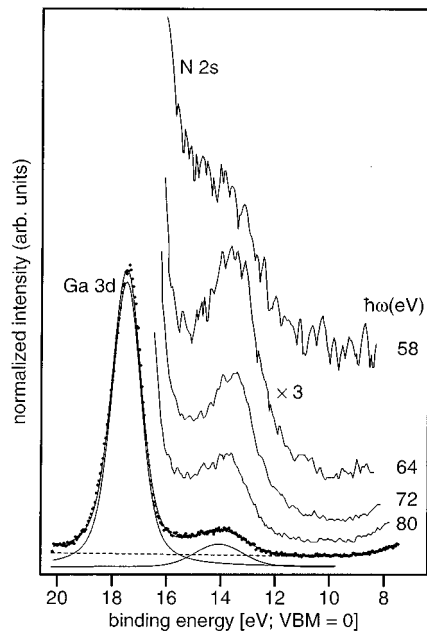


FIG. 5. Spectra in the Ga 3d/N 2s region from GaN (100). Also shown is a fit to the data based on two Lorentzian lines convoluted by Gaussians, with polynomial background (dashed line).

order polynomial was added to take the background (shown as a dashed line in Fig. 5) into account. The widths of the peaks were kept constant, and the intensity and peak energy were allowed to vary between different spectra. In this fashion the energy separation between the Ga 3d and the smaller peak was established. Since the Ga 3d peak had been found to be stationary in binding energy in separate experiments, this yields the dispersion of the smaller feature. Figure 6 shows a comparison of calculated bands in this region and our experimental results. The error bars represent the confidence intervals for the peak position that correspond to an

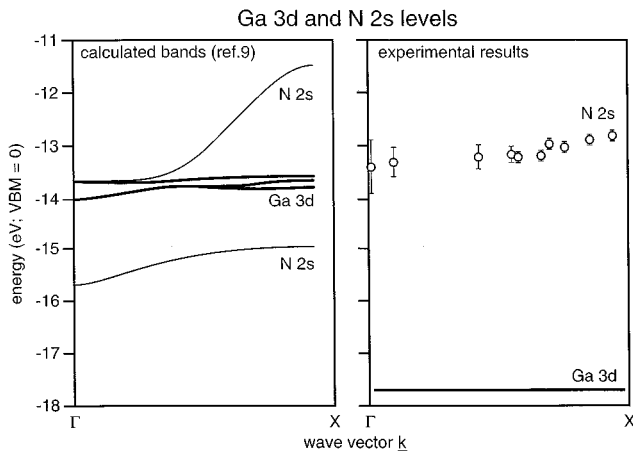


FIG. 6. Band structure along Γ -X in the region of the Ga 3d/N 2s bands. Lines are from the calculation of Ref. 9, while data points are evaluated from spectra similar to those in Fig. 5. Error bars represent the confidence intervals resulting from the fit (see the text).

increase of 1 in the χ^2 value. Theoretical data were taken from Fiorentini, Methfessel, and Scheffler.⁹ The experimental data yield a dispersion of the N 2s band of about 0.65 eV, and a separation between Ga 3d and N 2s of about 3.5 eV.

The calculated critical point energies of the Ga 3d–N 2s-derived bands are compared with the experimental results in Table I. There are discrepancies of up to about 4 eV in the position of these bands below the VBM. The general trend in the band calculations also shows a marked disagreement with experiment; agreement is good as far as the upper band edge is concerned, but the total amount of dispersion is overestimated by a factor 4–5 in the calculations. The close proximity of the N 2s and Ga 3d levels leads to a lower branch of the N 2s-derived band that disperses upwards and interacts with the Ga 3d level and an upper branch that continues the s-like dispersion of the N 2s level, such that emission from the N 2s-derived band is expected *below and above* the main Ga 3d peak (see Figs. 3 and 4 of Ref. 9).

However, this is not observed experimentally. Instead, a peak is only observed *above* the main Ga 3d peak; no intensity was detected below this peak (see Fig. 1). This can be explained in a simple two-level molecular orbital consideration by an energy separation of the Ga 3d and the N 2s levels; the separation is much larger than that resulting from the pseudopotential calculations, such that the hybridization is smaller, and due to the fact that the lower part of the hybrid state is close to the location of the Ga 3d peak, while the upper level is well separated from this level and only weakly interacts with the d states.

One has to keep in mind, however, that the above discussion neglects a vital point: the calculations report a ground state situation, while in the photoionization process correlation effects can play an important role, in particular for the flat Ga 3d bands. Lambrecht *et al.*¹⁷ have suggested that discrepancies may be due to self-energy corrections in these flat bands; however, Rubio *et al.*,¹³ in their comparison of the normal local density approximation (LDA) and quasiparticle (GW) calculations, arrive at self-energy corrections of about 1.5 eV for these bands (see Table I) that explain only part of the discrepancy. The small dispersion in the N 2s band also indicates that the separation between N 2s and Ga 3d is underestimated in the calculations: since the large dispersion is attributed not to direct overlap between adjacent N 2s orbitals but rather to an indirect interaction involving the Ga 3d levels, a larger separation and consequently a reduction in N 2s–Ga 3d interaction would lead to a smaller N 2s dispersion, as is found experimentally.

IV. SUMMARY

Angle-resolved photoelectron spectra from cubic GaN (100) and (110) films on GaAs (100) and (110) exhibit clear peak structure in the valence band region that is found to shift with photon energy, indicative of direct transitions between occupied and unoccupied GaN bands. The valence band dispersion along the Γ -X and Γ -K-X directions and the energy of critical points at the X point were determined. The relative energies of the Ga 3d and nitrogen 2s bands were

also studied, and a wider separation as well as a smaller amount of band dispersion than expected on the basis of calculations were found in the latter.

ACKNOWLEDGMENTS

The authors acknowledge the expert technical support by H. Haak and the help of the staff of the Berliner Speicherring Gesellschaft für Synchrotronstrahlung GmbH (BESSY). This work was supported through Bundesministerium für Bildung, Wissenschaft, Forschung und Technologie, as well as by the European Community through its International Cooperation Programme. One of the authors (J.H.W.) held an Alexander von Humboldt senior research award during his stay at the Fritz-Haber-Institute.

- ¹I. Akasaki and H. Amano, in *Wide Band Gap Semiconductors*, edited by T. D. Moustakas, J. I. Pankove, and Y. Hamakawa (Materials Research Society, Pittsburgh, 1993), p. 383.
- ²G. Martin, S. Strite, A. Botchkarev, A. Agarwal, A. Rockett, H. Morkoç, W. R. L. Lambrecht, and B. Segall, *Appl. Phys. Lett.* **65**, 610 (1994).
- ³Z. Q. He, X. M. Ding, X. Y. Hou, and X. Wang, *Appl. Phys. Lett.* **64**, 315 (1994).

- ⁴N. Kuwano *et al.*, *Jpn. J. Appl. Phys.* **33**, 18 (1994).
- ⁵O. Brandt, H. Yang, B. Jenichen, Y. Suzuki, L. Däweritz, and K. H. Ploog, *Phys. Rev. B* **52**, R2253 (1995).
- ⁶H. Yang, O. Brandt, and K. Ploog (unpublished).
- ⁷R. W. Hunt, L. Vanzetti, L. Castro, K. M. Chen, L. Sorba, P. I. Cohen, W. Gladfelter, J. M. Van Hove, J. N. Kuznia, M. Asif Khan, A. Franciosi, *Phys. B* **185**, 415 (1993).
- ⁸Landolt-Börnstein. *Electronic Structure of Solids: Photoemission Spectra and Related Data*, edited by A. Goldmann and E. E. Koch (Springer, Berlin, 1989), Vol. 23a.
- ⁹V. Fiorentini, M. Methfessel, and M. Scheffler, *Phys. Rev. B* **47**, 13 (1993).
- ¹⁰T. C. Chiang and D. E. Eastman, *Phys. Rev. B* **22**, 2940 (1980).
- ¹¹L. Sorba, V. Hinkel, H. U. Middelman, and K. Horn, *Phys. Rev. B* **36**, 8075 (1987).
- ¹²F. Solal, G. Jezequel, F. Houzay, A. Barski, and R. Pinchaux, *Solid State Commun.* **52**, 37 (1984).
- ¹³A. Rubio, J. L. Corkill, M. L. Cohen, E. L. Shirley, and S. G. Louie, *Phys. Rev. B* **48**, 11810 (1993).
- ¹⁴A. F. Wright and J. S. Nelson, *Phys. Rev. B* **50**, 2159 (1994).
- ¹⁵L. Wenchang, K. M. Zhang, and X. Xie, *J. Phys. Condens. Matter* **5**, 875 (1993).
- ¹⁶N. E. Christensen and I. Gorczyca, *Phys. Rev. B* **50**, 4397 (1994).
- ¹⁷W. R. L. Lambrecht, B. Segall, S. Strite, G. Martin, A. Agarwal, H. Morkoç, and A. Rockett, *Phys. Rev. B* **50**, 14 155 (1994).